ORIGINAL RESEARCH ARTICLE

Indoor tracking for smart hospital by a hybrid visible light positioning system

Zijin Pan[1], Jeremy Carleton[2], Sunny Zeng[2], Tian Lang[2], Gang Chen[2], Albert Wang[2,*]

[1] *Electrical and Computer Engineering, University of California, Riverside, CA 92521, USA*

[2] *University of California, Riverside, CA 92521, USA*

* Corresponding author: Albert Wang, aw@ece.ucr.edu

ABSTRACT

Modern hospital operations and management, i.e., smart hospitals, require pervasive system-wide wireless communication and positioning capabilities. Unfortunately, this cannot be entirely facilitated by existing radio frequency (RF) wireless technologies due to interference concerns in hospitals. We design and implemented a novel hybrid RF-free wireless tracking system utilizing combined visible light communication (VLC) and positioning (VLP), and powerline communication (PLC) technologies to enable future smart hospital operations. This VLC/VLP/PLC tracking system consists of host optical transceivers embedded in light-emitting diode (LED) bulbs and user-end photodetector (PD) optical tags, as well as backbone powerline interface, to form a ubiquitous wireless tracking and communication network connecting all people and equipment throughout all hospital buildings. The new indoor optical-based tracking system was validated via simulation and experiments. Being embedded into the existing LED lighting infrastructure, this hybrid VLC/VLP/PLC tracking system technology is accurate, ultralow cost and environment friendly. Smart hospitals will lead to efficient and affordable healthcare, a revolutionary solution in the human society.

Keywords: indoor positioning; indoor tracking; visible light positioning; VLP; visible light communication; VLC; powerline communication; PLC; LED

1. Introduction

Wireless communication and positioning technologies have altered our civilization as one of the fastest-growing application sectors. Countless mobile devices are now serving unlimited applications based on wireless technologies. Unlicensed optical wireless communications have recently been considered as an alternative to existing radio frequency (RF) communications and positioning/tracking methods. Nevertheless, RF-based indoor tracking and navigation technologies are still either unavailable or lack of precision for practical indoor positioning systems (IPS). Specially, in the healthcare settings, e.g., hospitals, where wireless is desired, visible light communication (VLC) and positioning (VLP) technologies have numerous potentials. In general, RF wireless is often forbidden in critical wards in hospitals since strong RF interferences may be life-threatening due to interferences to various medical devices, such as healthcare equipment or a pacemaker wore by a patient[1]. It is expected that future hospitals and healthcare facilities will go smart by implementing various smart technologies and devices. Particularly, a hospital is a large physical setting with complex human-building-instrument interactions that requires management efficiency. Hence, we envision that smart hospital

operations are needed for future healthcare systems. Simply imagining the number of actors (doctors, nurses, patients and visitors) involved in daily activities in a hospital, the large volume of various medical instruments needed for medical care, and the complex layout of hospital buildings, therefore, managing a large hospital in real world efficiently is never an easy task. Being able to instantly and accurately tracking all actors, devices, buildings, rooms and their interactions in a hospital is the basis for smart hospital operations in future, which requires reliable wireless indoor tracking technologies, as well as hardware and software systems. To address this critical need for smart hospital operations in an indoor environment without relying on RF wireless technologies, we proposed and designed an LED-based VLC/VLP technology platform to realize a low-cost, low-complexity indoor tracking system for smart hospitals. Numerous existing studies have explored various types of VLP technology, employing different positioning algorithms, numbers of LEDs, and sensors[2–4]. Several VLP systems boasting centimeter-level accuracy have been reported in recent years, making them potential candidates to address the aforementioned problem in hospitals. The innovation of our project is that the hybrid VLP/PLC tracking system we proposed incorporates VLP technology and employs PLC to gather information from multiple LEDs, which is then automatically displayed in the GUI with the user's position. It utilizes the existing LED lighting infrastructure in a hospital to realize an energy-efficient visible light based tracking system. Basically, the new generation of solid-state LED light bulbs can be electrically modulated to achieve VLC/VLP functions for both optical wireless communications and positioning. Since the LED modulation speed is very high, no light flickering will be sensed by human eyes. Therefore, the existing LED lighting infrastructure will support indoor optical positioning and communications to enable real-time and precise asset and person tracking, therefore, facilitating smart hospital operations, which not only can support healthcare quality, but also will dramatically reduce healthcare costs by making hospital operations more efficient. This LED VLC/VLP system allows for big data collection, development of user-hospital-building interaction models, and implementation of artificial intelligence (AI) algorithms for future smart hospital operations[5–8]. In this work, visible light, infrared (IR) light and powerline communications are combined to provide a VLP functions within a building and support infrastructure-wide data communications for large-scale smart hospital operations. This paper is an extended version of a conference presentation[9].

2. System overview

The new LED-based VLC/VLP system utilizes two unidirectional lines of communications to achieve bi-directional communications between the tracked users (e.g., actors, medical devices) and light fixtures housing LED bulbs. For the first line of communication, a fixture uses on-off keying to transmit data through the visible light emitted from LEDs. The LEDs can be either existing LED light bulbs or specially designed LED optical tags. The presence or absence of the carrier frequency is determined by filtering the output of a photodiode (i.e., PD, serving as a photodetector) on the user end. The information that the user receives through this line of communication includes both the ID of the fixture sending the signals and its proximity to that fixture, which is derived from the received signal strength (RSS). For the second line of communication, infrared (IR) signals are transmitted by the user and decoded by one or more LED fixtures. IR light is used to avoid uncomfortableness to human eyes in practical settings. The information that the lighting fixtures receive through this line of communication is the horizontal distance between the user and the last fixture that transmitted a signal. The main goal of these communications is to supply the graphical user interface (GUI) software with the information required to triangulate the user's position within the floorplan of a room or building, although data for other purposes can be communicated as well. A way to bring this information to the GUI is to have all fixtures connected to a backbone powerline in a large building, existing for lighting infrastructure in buildings, which enables powerline communications with the GUI through a hospital.

3. System design

In our prototype VLC/VLP system, each fixture consists of a four-by-four array of commercial LEDs, an infrared receiver, an Arduino Uno microcontroller with an ethernet shield, an amplifier circuit used to drive the LEDs with 28 V, and a connection to the powerline through a Powerline 500 AV Nano Adapter. On each fixture, the LEDs and infrared receiver are outward-facing and directed towards the ground, while the other components (excluding the powerline adapter) are contained within an enclosure. **Figure 1** shows the layout of the LEDs on the bottom of a fixture. **Figure 2** depicts the block diagrams of the tracking fixture units and the device used to track a user. On the tracking fixtures, the microcontroller controls the LEDs with a 5 V digital signal applied to the gate of a MOSFET, which drives the LEDs using 28 V supply. As seen in **Figure 2**, the user device contains two microcontrollers, an Arduino Due and an Arduino Nano, which separately handle receiving visible light signals and transmitting infrared light signals. A pair of identical photodiodes receive the visible light signals and produce currents, which are input into a VSOP383 preamplifier and a transimpedance amplifier (TIA), respectively. The VSOP383 preamplifier includes a bandpass filter to allow for detection of the carrier frequency. The output of the VSOP383 preamplifier is a digital signal that provides the binary data transmitted by a fixture (Section 4).

Figure 1. The underside of a tracking fixture unit. Infrared receiver not included.
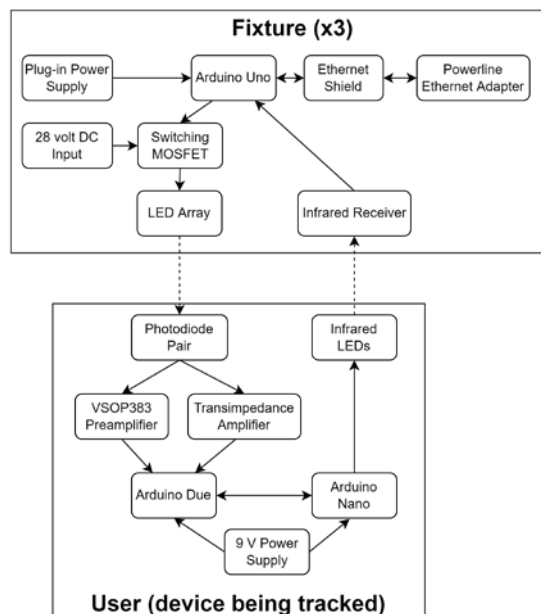
Figure 2. Block diagrams for the VLC/VLP tracking fixtures and the tracked device.

This signal is input to a digital pin on the Arduino Due. The TIA produces a waveform centered on 1.65 V, which oscillates when one of the fixtures is transmitting the carrier frequency. This signal is input to an analog pin on the Arduino Due and is used to determine the received signal strength (Section 6). The Arduino Nano transmits data back to the fixtures using infrared LEDs after receiving the data to be transmitted from the Arduino Due. The data is encoded using the NEC protocol with a 38 kHz carrier frequency. In each response that the user transmits to the fixtures, the ID of the fixture that was transmitting and the distance calculated are transmitted in a total of four NEC messages, each of which contain two bytes. The distance is given in units of millimeters and represented using the 32-bit IEEE floating point format. The IRREMOTE library version 3.6.1 for Arduino is used to both generate and decode infrared signals.

4. VLC tracking theory and implementation

In this section, we will discuss the tracking theory employed, providing detailed information on the modulation of signals and the modeling of the relationship between the RSS and the distance between the light fixture and the photodiode (the user's position). Subsequently, we delve into the calibration of distance, covering both the theoretical aspects and the corresponding experimental data.

On-off keying (OOK) modulation was employed to encode the ID of a fixture into its visible light signals, each LED fixture's microcontroller can alternate between outputting a constant voltage and outputting a 38 kHz square wave on the pin, which drives the gate of the switching MOSFET. When sending a zero ("0") bit, the microcontroller outputs the constant voltage. When sending the one ("1") bit, the microcontroller outputs the 38 kHz square wave. This encoding method is advantageous because a fixture's LEDs will never turn off for longer than 13.16 ms for any combination of data bits being sent. This ensures that no perceptible flickering will occur, which could disturb persons in a room lit by the fixtures.

To receive the optical bits transmitted by a fixture, the Arduino Due on the user device waits for a start bit of one ("1") to be received by setting an interrupt on the pin connected to the VSOP383 preamplifier. The preamplifier output is at the high logic level ("H") by default and switches to the low logic level ("L") only when the 38 kHz carrier frequency is detected. Thus, the start bit is signified by a falling edge on the pin that triggers the interrupt. The microcontroller then waits for the first data bit to begin and samples the same input pin halfway through receiving the bit to determine if the bit is a "1" or a "0". This process is repeated for all eight data bits in the byte word received. The last bit in the byte of data is followed by a "1", which is the stop bit.

In applications where only visible light positioning is required (i.e., the only information that a fixture needs to communicate is its ID), only a single byte word is sent. If additional data needs to be communicated, a short idle period where the fixture transmits a zero bit is needed, after which the next byte can begin.

Figure 3 breaks down the sequence and timing for sending one or more bytes of data. The start bit for the first byte transmitted needs to last 2000 ms to provide the user with sufficient time to collect the samples used to determine the received signal strength. All other bits last for 300 ms. The total time required to send the first byte in a sequence is 4700 ms, and for consecutive bytes it is 3000 ms.

While the signal from the photodiode is being translated into a digital signal by the VSOP383 preamplifier, it is also being amplified as an analog signal by the transimpedance amplifier. An analog to digital converter (ADC) built into the microcontroller samples the output from the transimpedance amplifier 1000 times during the start bit to measure the signal's average peak-to-peak (p-p) amplitude (A_{p-p}). Because the DC component of the signal from the PD is removed by the TIA, light produced by non-fixture sources should have no effect on the measured amplitude so long as it changes with a frequency significantly less than 38 kHz.
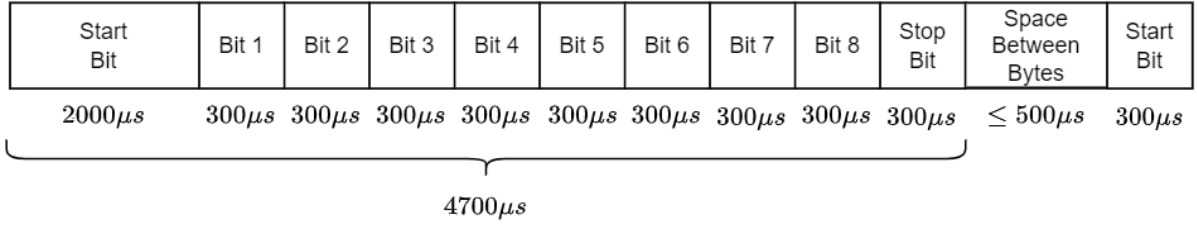
Figure 3. Sequence and timing of bits transmitted by a tracking fixture when multiple bytes are transmitted. The second byte is shown truncated after the start bit. When there are no consecutive bytes, the transmission ends after the first stop bit.

The average *p-p* amplitude across the 1000 samples is determined by taking the average of all values at peaks of the wave (p_i) and subtracting the average of all values at troughs of the wave (t_i). This is shown in Equation (1). The average *p-p* amplitude is A_{p-p} and the number of peaks and troughs counted are n_p and n_t, respectively.

$$A_{p-p} = \frac{\Sigma p_i}{n_p} - \frac{\Sigma t_i}{n_t} \tag{1}$$

Once the microcontroller determines the transmitting fixture's contribution to the overall light intensity received by the photodiode, it estimates the distance between the photodiode (the user's position) and the transmitting fixture. Since the goal is to locate the user within a two-dimensional map of a room, the distance in the z-direction (vertical) must be removed from the final estimate. Since all fixtures are mounted on the same ceiling in a room with the same height above the ground, this distance is the same regardless of which fixture is transmitting.

The existence of a relationship between RSS and proximity to a signal's source is well-documented in existing literature. For example, an optical channel model used in study of Zhang et al.[10] could be applied to relate the RSS to the distance between the fixture and the user. This model accounts for only the line-of-sight propagation path of light from the emitter to the receiver. The channel DC gain is given as,

$$H(\phi, \psi, d) = A \cdot T_s(\psi) \cdot g(\psi) \cdot \frac{m+1}{2\pi d^2} \cdot \cos^m(\phi) \cdot \cos(\psi) \tag{2}$$

where ϕ is the angle from the normal vector of the fixture to the path taken by the light from the emitter to the receiver, ψ is the angle of incidence, and d is the Euclidean distance between the emitter and the receiver (**Figure 4**). Furthermore, A is the area of the sensor detector, $T_s(\psi)$ represents the optical filter gain, $g(\psi)$ represents the concentrator gain, and m is the Lambertian order of the emitting light source.

The distance d is the hypotenuse of a right triangle with legs d_{xy} and d_z, where d_{xy} is the component of the distance along the ground plane and d_z is the vertical component of the distance. By the Pythagorean theorem, we have

$$d = \sqrt{\left(d_{xy}\right)^2 + (d_z)^2} \tag{3}$$

Since the distance between LEDs in the same fixture is small compared to d_z, the distances between individual LEDs and the photodiode are approximately equal. As a result, we treat each fixture as a single light source with the combined optical power output of the sixteen LEDs on one LED panel used. This can be seen in **Figure 4**.
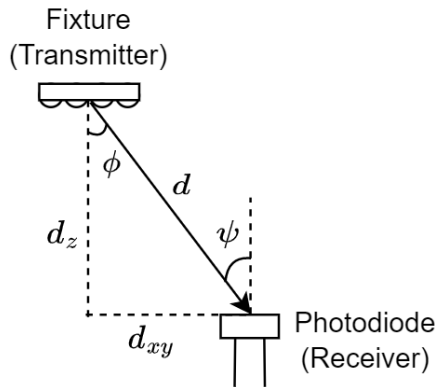
Figure 4. Geometric quantities involved in determining the optical channel DC gain.

From in study of Kahn and Barry[11], the concentrator gain $g(\psi)$ is a constant determined by the characteristics of the receiver for all ψ within the field of view of the receiver's concentrator. The optical filter gain $T_s(\psi)$ also depends on constant characteristics for a given receiver, and we approximate it with a constant for all ψ within the field of view. As a result, for all cases where ψ is less than the field of view semi-angle, the product of A, $T_s(\psi)$, and $g(\psi)$ can be reduced to a constant K.

$$A \cdot T_s(\psi) \cdot g(\psi) = K \tag{4}$$

For all other values of ψ, the received signal will be too weak to perform a distance calculation.

The optical channel model is further simplified by the fact that the photodiode points directly upward towards the ceiling on which all fixtures are mounted. This means that the angles ψ and ϕ are equal and depend only on the distance d_{xy}. In particular, we have the following relationship.

$$\cos(\psi) = \cos(\phi) = \frac{d_z}{d} \tag{5}$$

Using Equations (3)–(5), and assuming the Lambertian order of the LEDs to be one, we can rewrite Equation (2) with d_{xy} as the only value that is variable.

$$H(d) = \frac{K(d_z)^2}{\pi \left[\left(d_{xy} \right)^2 + (d_z)^2 \right]^2} \tag{6}$$

Although Equation (6) provides a basis for modeling the relationship between RSS and the distance d_{xy} that is needed for triangulation, estimating the appropriate value to use for K can be problematic. Furthermore, the assumption that the Lambertian order is one may not hold true for all lighting systems. To eliminate this difficulty, calibration is performed under conditions similar to those under which the system needs to operate in a real world. This is done by measuring A_{p-p} while varying the distance between the fixture and the photodiode. This method assumes that the photodiode will maintain a fixed height relative to the fixtures at all times during both the calibration process and regular operation.

We performed calibration for each fixture using the following method: the photodiode, the transimpedance amplifier (TIA), and the Arduino Due for the user were fixed to a slider that could move along one axis. A motor was used to automatically pull the slider at a low speed in order to vary the distance between the photodiode and the fixture. Measurements were taken for every six millimeters (mm) that the photodiode moved. A total of 72 measurements could be taken before the slider needed to be reset, for a distance of 432 mm. To take measurements at farther distances, the starting point of the slider was moved further away from the fixture in increments of 305 mm (1 ft).

At each measurement point, the Arduino Due took 1000 samples of the signal from the TIA using its ADC and computed A_{p-p} using Equation (1). To avoid spending time converting to units of volts, A_{p-p} is expressed in terms of LSBs of the ADC output where each LSB corresponds to approximately 806 μV.

Figure 5 shows a set of calibration data collected for d_{xy} ranging from 0 m to 2.864 m. Each data point is marked as a blue dot and indicates an average amplitude measurement obtained at a specific distance from the fixture. Superimposed onto the data is a piecewise linear function consisting of 13 line segments, shown in black. Each line segment covers a different interval of the x-axis and was chosen to fit the data on that interval. The equation for each line segment is of the form:

$$d_{xy} = c_1 \cdot A_{p-p} + c_2 \tag{7}$$

where c_1 and c_2 are constants determined using the MATLAB Curve Fitting Toolbox. Together, these equations are used to model the relationship between signal amplitude (A_{p-p}) and distance (d_{xy}), so that the distance can be quickly computed on the Arduino Due.

The complete procedure used to calculate the distance d_{xy} is as following: first, the program running on the Arduino Due calculates the average amplitude of the set of 1000 samples with the same algorithm used during calibration. Next, the program determines which values of c_1 and c_2 to use based on what interval the value of A_{p-p} falls into. Finally, the program calculates d_{xy} using Equation (7).
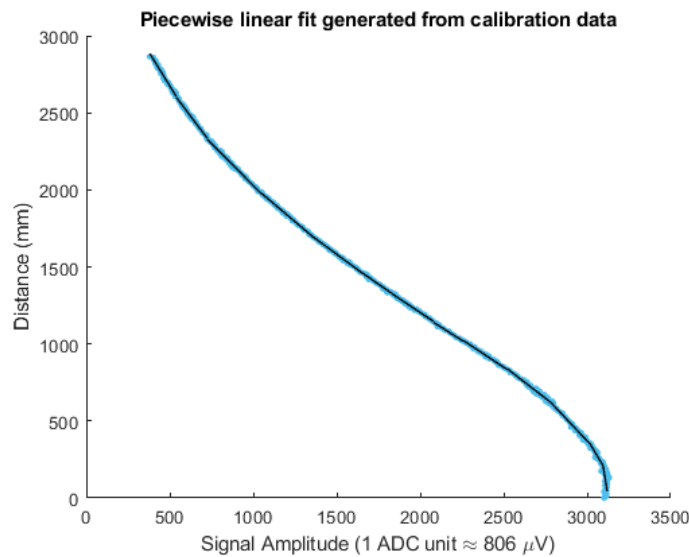
Figure 5. Scatter plot of the full set of calibration data collected for a single fixture, with the piecewise linear function (black line) used to fit the data (blue dots).

## 5. Integration with power-line communication

The powerline communication portion of this project has allowed the design of a hospital-wide system (i.e., a large campus with many buildings) for communications with existing LED lighting infrastructure. Using Powerline 500 AV Nano Adapters, an ethernet network is extended over the existing powerline used to supply power to the lighting fixtures. This network connects each fixture to a single Arduino Uno, which also uses an ethernet shield. This microcontroller acts as a proxy for the computer running the GUI applications by collecting incoming data from the fixtures and providing updated distance measurements to the computer when they are available. During system startup, the proxy microcontroller establishes an ethernet server that the microcontroller on each fixture connects to. Fixtures on the network are distinguished based on their unique IDs and IP addresses. The Arduino Ethernet library is used for communications between microcontrollers over the ethernet network.

In addition to its role as a proxy for the GUI subsystem, the microcontroller running the ethernet server has complete control over when each fixture transmits data, allowing it to coordinate the fixtures to efficiently communicate while avoiding overlap in the transmission of visible light signals.

6. GUI subsystem

An essential component in the Connected Smart Hospital project is the graphical user interface tracking/mapping subsystem. The objective of the graphical user interface is to implement the front end of the project, providing three main features: data input, data processing, and data output. These three features are implemented and interface with the graphical user interface using Python. The graphical user interface subsystem receives data from visible light tracking through the utilization of powerline communications. The data is transmitted to the computer system through UART and logged into a CSV file, which is readily accessed via Python. The primary contents of the data include the distance of a user relative to three different lighting fixtures to facilitate data processing and output; the graphical user interface subsystem processes user data through triangulation of the aforementioned distance data obtained from powerline communications. The triangulation process is accomplished by utilizing Python Descartes and Shapely libraries. Through the utilization of the polygon and geometry functions of Descartes and Shapely, the region of intersection of the distance data can be triangulated and plotted.

The final feature of the graphical user interface subsystem data output is accomplished through Python using the Tkinter library. The graphical user interface implements a window including all relevant light fixture data, plotting the triangulated data, as shown in **Figures 6** and **7**. The graphical user interface automatically reads the data from the CSV file and updates the plot with the user positions in rectangular coordinates. The user position is defined by the intersection of three LED intensity rings formed by calculating the distance data from the CSV file with an error constrain value defined in Python. **Figure 8** shows the region of intersection with the three LED intensity rings. The tracking results will be further used to construct a tracking map showing all actors and equipment to be monitored in a hospital, overlaying the given campus and building layout map to facilitate smart tracking and operations.
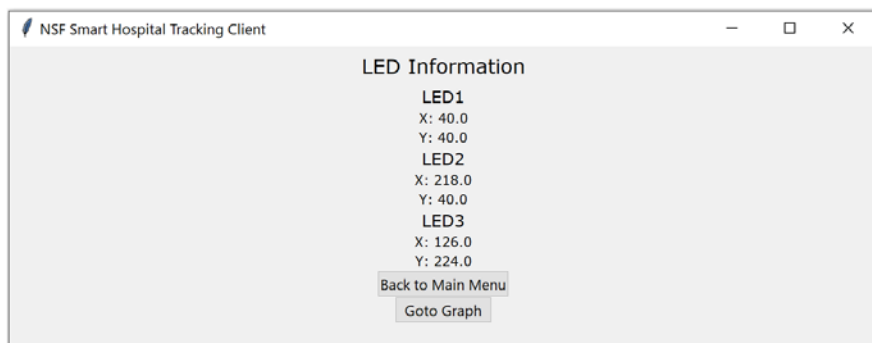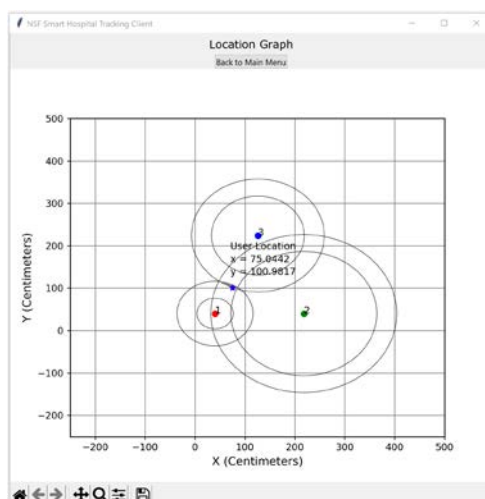

Figure 6. A graphical user interface window displaying the LED positions.
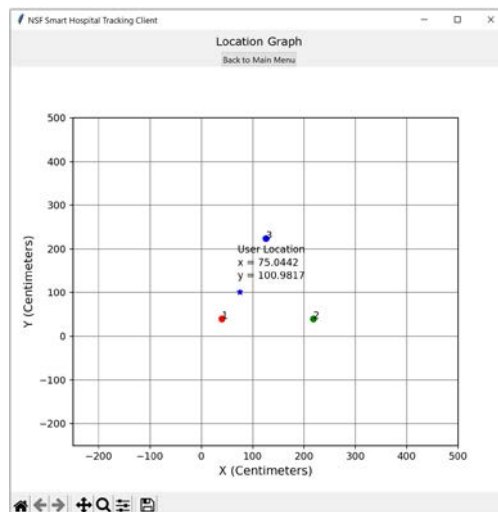
Figure 7. Graphical user interface displays the user position function. Triangulation is used to get a region of intersection.

Figure 8. GUI shows exemplar user position as (75.0442, 100.9817) with the distance of 562.91 mm, 1663.95 mm, and 1131.54 mm from LED 1, 2 and 3.

7. Summary of system performance

We have evaluated our VLC/VLP/PLC tracking system in terms of the accuracy of distance measurements between the user and an individual fixture, as well as the rate at which new location estimates are produced. We found that distance measurements are generally accurate to within 10 cm, although the accuracy may degrade when the user is within 50 cm of the transmitting fixture. When the system is running continuously, a new location estimation consisting of a distance for each of the three fixtures is added to the CSV file at least once every 1.7 s. The refresh rate for the GUI was set to 1 s in order to align with the required update rate of the CVS file.

To eliminate the interference from ambient light, the visible light and infrared signals were modulated using a 38 kHz carrier signal, so that the interference from ambient light can be eliminated by filtering only the 38 kHz signals at the receiver. However, in practical, it is essential to keep the ambient light stable and low enough to ensure the accuracy of the system. This is because excessive ambient light can cause the photodiode to saturate, leading to very noisy measurements. Additionally, anything obstructing the line of sight between the user and the light fixtures would invalidate the distance measurements.

8. Conclusion

We present the design and implementation of a novel hybrid visible light and powerline communications technology enabled indoor positioning system for smart hospital operations. The new RF-free indoor all-optical tracking system includes host LED lighting bulbs, user-end optical tags, and a PLC interface. Utilizing triangular LED positioning algorithms and distance calibration data, we achieved centimeter-level tracking accuracy. The GUI subsystem visually displays the user location in a tracking map with auto refreshment. The new VLC/VLP tracking system has been experimentally validated. ICs for this VLC/VLP tracking system are designed and will be fabricated in a 45 nm SOI CMOS technology. This hybrid VLC/VLP/PLC optical wireless monitoring system can potentially revolutionize hospital operations, leading to smart cost-effective healthcare in future.

Author contributions

Conceptualization, AW; methodology, GC and TL; software and validation, JC and SZ; formal analysis and investigation, ZP; resources, GC; data curation, TL; writing—original draft preparation, ZP; writing—review and editing, AW; supervision, AW; project administration, GC and TL; funding acquisition, AW. All authors have read and agreed to the published version of the manuscript.

Acknowledgments

Conflict of interest

The authors declare no conflict of interest.

References

1. Pan Z, Lang T, Li C, et al. Visible light communication cyber-physical systems-on-chip for smart cities. *Journal of Communications* 2019; 14(12): 1141–1146. doi: 10.12720/jcm.14.12.1141-1146
2. Zhuang Y, Yang J, Qi L, et al. A survey of positioning systems using visible LED lights. *IEEE Communications Surveys & Tutorials* 2018; 20(3): 1963–1988. doi: 10.1109/COMST.2018.2806558
3. Huang L, Wen S, Yan Z, et al. Single LED positioning scheme based on angle sensors in robotics. *Applied Optics* 2021; 60(21): 6275–6287. doi: 10.1364/AO.425744
4. An F, Xu H, Wen S, et al. A tilt visible light positioning system based on double LEDs and angle sensors. *Electronics* 2021; 10(16): 1923. doi: 10.3390/electronics10161923
5. Dong Z, Lu F, Ma R, et al. An integrated transmitter for LED-based visible light communication and positioning system in a 180 nm BCD technology. In: Proceedings of IEEE Bipolar/BICMOS Circuits and Technology Meeting (BCTM); 28 September–1 October 2014; Coronado, USA. pp. 84–87.
6. Lang T, Pan Z, Ortiz N, et al. Integrated design of low complexity RSS based visible light indoor positioning and power line communication system for smart hospitals. In: Proceedings of IEEE International Conference on Consumer Electronics (ICCE); 10–12 January 2021; Las Vegas, USA. pp. 1–5.
7. Kalay YE, Sathyanarayanan H, Schaumann D, et al. Simulation-powered smart buildings management enabled by visible light communication. In: Proceedings of the 11th Annual Simposium on Simulation in Architecture and Urban Design (SIMAUD); 25–27 May 2020; Online. pp. 1–8.
8. Lang T, Li Z, Lu F, et al. LED-based visible light communication and positioning technology and SoCs. In: Proceedings of 2018 14th IEEE International Conference on Solid-State and Integrated Circuit Technology (ICSICT); 31 October–3 November 2018; Qingdao, China.
9. Pan Z, Carleton J, Zeng S, et al. Design implementation of a hybrid VLP/PLC-based indoor tracking system for smart hospitals. In: Proceedings of IEEE International Conference on Consumer Electronics (ICCE); 6–8 January 2023; Las Vegas, USA. pp. 1–3.
10. Zhang W, Chowdhury MS, Kavehrad M. Asynchronous indoor positioning system based on visible light communications. *Optical Engineering* 2014; 53(4): 045105. doi: 10.1117/1.OE.53.4.045105
11. Kahn JM, Barry JR. Wireless infrared communications. *Proceedings of the IEEE* 1977; 85(2): 265–298. doi: 10.1109/5.554222